Title

HIGH TEMPERATURE ELECTRICAL CONDUCTIVITY OF NON-STOICHIOMETRIC GADOLINIUM-GALLIUM GARNET SINGIE CRYSTALS

Authors

Donaghey, L.F.
Wright, Conrad L.

Publication Date

1973-10-01

Submitted to J. Physics and
Chemistry of Solids

LBL-2244
Preprint

c. 1

HIGH TEMPERATURE ELECTRICAL CONDUCTIVITY OF NON-STOICHIOMETRIC GADOLINIUM-GALLIUM GARNET SINGLE CRYSTALS

L. F. Donaghey and Conrad L. Wright

October 1973

Prepared for the U.S. Atomic Energy Commission
under Contract W-7405-ENG-48

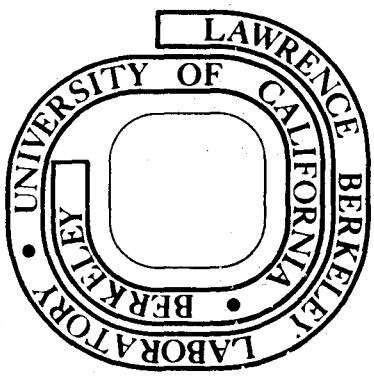

LBL-2244

DISCLAIMER

High Temperature Electrical Conductivity of Non-stoichiometric Gadolinium-Gallium Garnet Single Crystals

L. F. Donaghey and Conrad L. Wright†

Inorganic Materials Research Division of the
Lawrence Berkeley Laboratory and the
Department of Chemical Engineering of the
University of California, Berkeley
Berkeley, California 94720

Abstract

The electrical conductivity of single crystal gadolinium-gallium garnet in the [211] direction was measured in the temperature interval from 1073 to 1700 °K and in oxygen partial pressures from 10^{-18} to 1 atm. Intrinsic, doubly ionized anion vacancy defects predominate at high temperatures (above 1538 °K at P_{O_2} = 1 atm), with an activation energy for conduction of 5 eV. Below approximately 1538 °K the extrinsic conductivity is n-type with an apparent activation energy of 2.60 ± 0.11 eV. The conduction mechanism in the extrinsic region is probably controlled by triply ionized gallium and aluminum interstitials introduced during Czochralski crystal growth.

---

†Present Address: Hewlett-Packard Co., 1501 Page Mill Rd., Palo Alto, California.

Introduction

Gadolinium gallium garnet ($Gd_3Ga_5O_{12}$ or GGG) is an important substrate material utilized in the epitaxial growth of garnet thin films for application in magnetic bubble domain memories. The absence of ferromagnetism in this compound, the high optical transmission throughout the visible spectrum, and the lattice parameter comparable to that of ferrimagnetic, rare-earth substituted garnets make this compound an ideal substrate material for magneto-optical thin film device applications. As defect structures in the substrate material can interact with the magneto-optical properties of epitaxial thin films, a knowledge and thorough characterization of the defect structure in GGG is important to the success of device applications. Lack of control over cation stoichiometry during crystal growth can lead to precipitation of secondary phases during annealing, while divalent or tetravalent impurities in the source chemicals or introduced by contamination during crystal growth can stabilize point defects in the lattice and produce unwanted consequences in optical and magnetic properties.

The electrical properties of garnets and orthoferrites are potentially useful as a semi-quantitative method for determining their chemical purity with respect to impurities which compensate magnetic ions (1). When chemically stoichiometric the magnetic garnets and orthoferrites are highly insulating with room temperature resistivities in excess of 10^{12} ohm-cm . When these crystals are doped with di- and tetravalent ions, however, the resistivities

drop markedly to as low as 10^4 ohm-cm with as little as 10^{-3} impurity moles per formula mole (2). Thus, the measurement of electrical resistivity can be employed in assessing the impurity content in solution grown and chemically vapor deposited magnetic oxide films.

Electrical transport studies have yielded useful information about the density of lattice defects (4). In the literature, however, there are few reports on the electrical conductivity of rare-earth oxides. Tare and Schmalzreid (5) have reported predominantly ionic conductivity in rare-earth sesquioxides while Noddack and Walch (6) have found electronic conduction to predominate in several rare-earth oxides. The effect of Sn doping on the electrical conductivity of Gd and Tm orthoferrites was studied by Wood et al. (2). These authors report a decrease in the room temperature electrical resistivity from $\sim 10^{12}$ to $\sim 10^4$ ohm-cm with increasing Sn concentration.

The effects of Ca^{2+} and Si^{4+} ion doping on optical and electrical properties of YIG were studied by Wood and Remeika (3). These ions produce charge compensating Fe^{4+} and Fe^{2+} ions, respectively, from the normally Fe^{3+} ions, thereby increasing the electrical conductivity by an electron hopping mechanism. The electrical resistivity for both Ca and Si doping decreases linearly with impurity concentration to $\sim 10^6$ ohm-cm for 0.002 impurity atoms per formula. Further increase in impurity content, however, causes a change in point defect equilibrium or in the conduction mechanism, as the electrical conductivity becomes assymptotic

to $\sim 10^5$ ohm-cm . The conductivity is p-type with Fe^{4+} ions, and n-type with Fe^{2+} ions present, as determined by means of the thermoelectric effect. Electronic conduction in rare-earth containing garnets undoubtedly involves the 4f-electrons, and the width of the band gap should be related to the number of filled 4f-shell orbitals (7).

In the present study the conductivity of Czochralski-grown single crystal GGG was studied as a function of temperature and oxygen partial pressure in order to establish the defect equilibria, the activation energies for conduction, and the conduction mechanism.

Experimental

The $Gd_3Ga_5O_{12}$ single crystal material used in this study was prepared from 99.999% Ga_2O_3* and 99.9% Gd_2O_3† powders which were induction heated in an Ir crucible within a ZrO_2 enclosure containing a $N_2 - O_2$ gas mixture containing .0015 to .002 atm O_2.†† A stainless steel seed hold was used to support a <111> orientation crystal of $Gd_3Ga_5O_{12}$. Crystal growth of a 2 cm diameter crystal by the Czochralski process was then carried out at a rate of 1/8 inch/hr. The major source of impurity elements in the final crystal is the Gd_2O_3 source chemical. The major impurities in this reagent are other rare-earth oxides. According to the supplier, the

---

*Allusuisse, Switzerland

†Research Chemicals, New York, N.Y.

††Union Carbide Corp., San Diego, California

concentration of the major tetravelent ion, silicon, is less than .005% by weight of oxide, and that of the major divalent ion, cooper, appears in a lower concentration.

Single crystal specimens with dimensions 0.1 cm × 0.2 cm × 1.8 cm and with the axis of the long dimension parallel to the [110] crystallographic direction were cut from a single crystal grown from the melt by the Czochralski process. The results of an emission spectrographic analysis of the single crystal source material is summarized in Table 1. The specimens were polished to a 1 micron finish using successively finer grades of silicon carbide laps and diamond paste. After thorough washing of the samples, residual organic material was removed with ethyl alcohol followed by warm air drying. The specimen was then mounted in the conductivity apparatus shown in Fig. 1 with 0.010 in. diam. standard grade platinum wires wrapped around the ends of the specimen to form the current leads, and 0.005 in. dia. platinum wires spaced 1 cm apart wrapped around the sample between the current leads to form potential probes.

Electrical conductivity measurements were performed using a four point probe d.c. technique with a PAR Model 162 electrometer and standard voltage cell within a completely shielded circuit shown in Fig. 2. High isolation, low conductivity reed switches were employed to isolate the current and voltage circuits of the cell and to allow sequential measurement of both current and voltage with the same electrometer. The partial pressure of oxygen within the cell was controlled by a mixture of pure gases to form a dynamic atmospheres

Table 1.

Mass Emission Spectrographic Analysis* of Czochralski-grown, Single Crystal $Gd_3Ga_5O_{12}$

element	concentration as oxides (ppmo)
Ga	Principal constituent
Gd	Principal constituent
Al	40 ppm
Ir	N. D.† (0.05%)
Pb	N. D.† (<100 ppm)
Si	N. D.† (<.005)
Sn	N. D.† (<0.01%)
Ca	N. D.† (0.002%)

*American Spectrographic Laboratories, Inc., San Francisco, California.

†Not detected. The limit of detectability is given in parentheses.

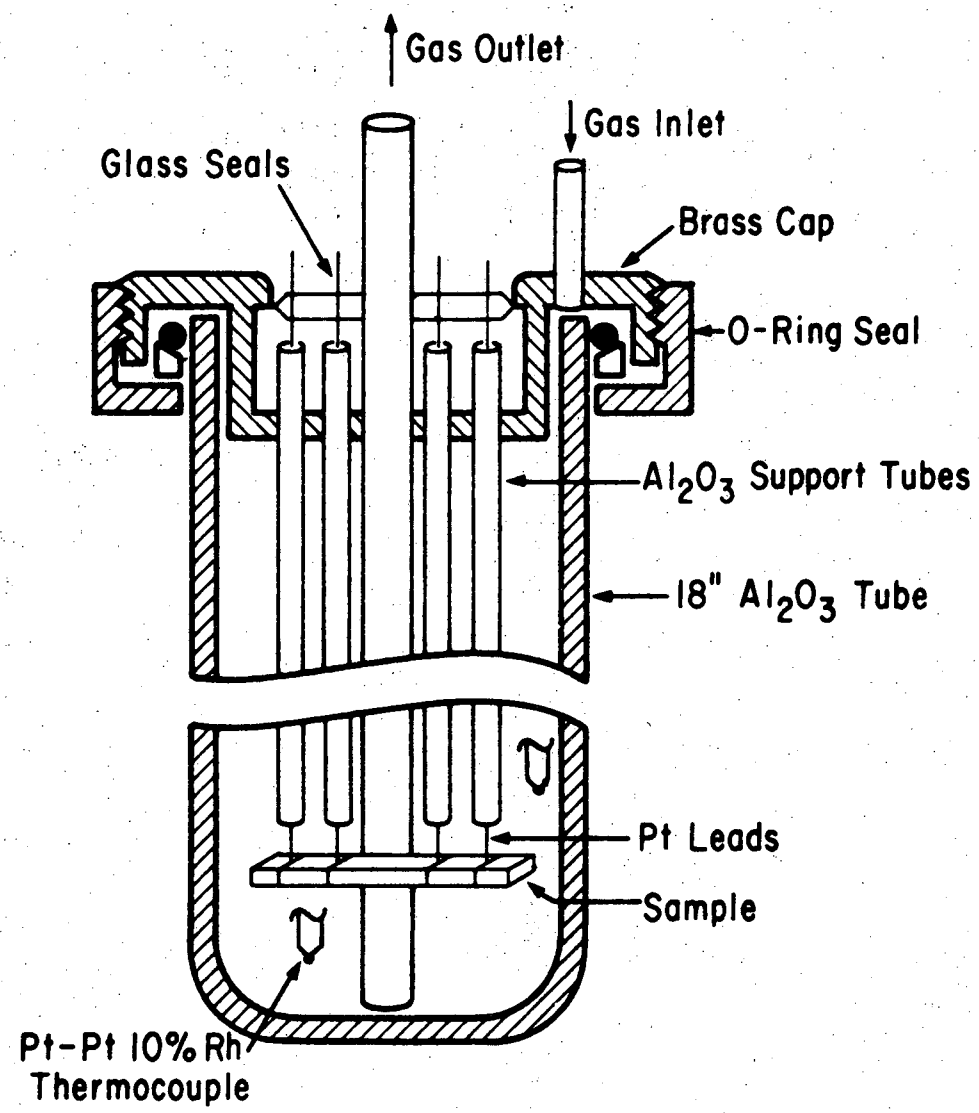

XBL739-1888

Figure 1. Experimental cell showing orientation of the oxide sample

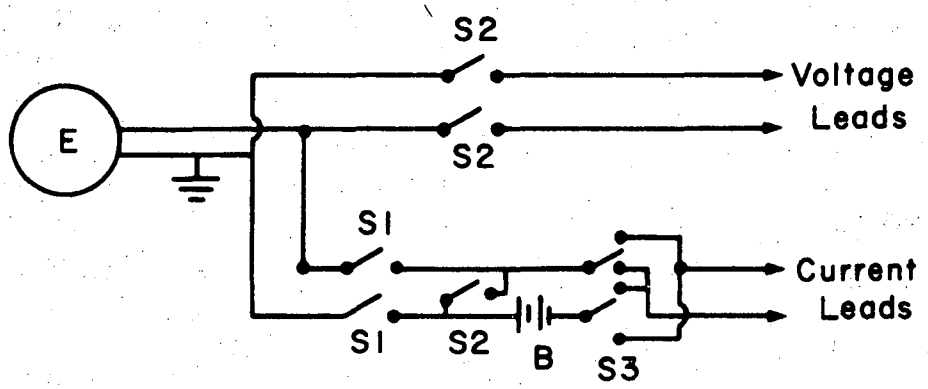

B = 10.5 V Battery
E = Electrometer
S1 = Reed switches, closed for current measurement
S2 = Reed switches, closed for voltage measurement
S3 = Current reversing switch

XBL739-1889

Figure 2. Electrical circuit for four point conductivity measurements

of pure oxygen, oxygen-argon mixtures, carbon dioxide-argon mixtures, and mixtures of carbon monoxide and carbon dioxide. The thermal diffusion effect was minimized by maintaining a gas flow velocity of 1 cm/sec with all gases individually calibrated for each gas (8). The gases were mixed in a packed column containing glass spheres prior to entry into the conductivity cell. The partial pressures for various gas mixtures was calculated from known thermochemical data (9). Several regions of the P_{O_2} - T diagram are inaccessible with O_2 - Ar - CO - CO_2 gas mixtures, and require special buffers for achieving desired oxygen partial pressures. The inaccessible ranges in log P_{O_2} increase with decreasing temperature.

Measurement of conductivity was carried out at various temperatures between 1073 °K and 1700 °K in the following manner:

Following equilibration at a specified temperature the reed switches connecting the electrometer to the current probes were closed, applying a potential across the sample. The potential drop along the sample was then measured by opening the current circuit reed switches, then closing the reed switches in the potential circuit. The direction of current flow was then reversed and the measurements repeated. Conductivities were measured at equilibrium states approached from higher oxygen partial pressures as well as from lower partial pressures to provide a check on the state of equilibrium.

Results and Discussion

The dependence of the electrical conductivity of $Gd_3Ga_5O_{12}$ on reciprocal absolute temperature is shown in Fig. 3 for fixed mixtures of $Ar - O_2$ and $CO - CO_2$. The slopes of these functions is insensitive to either gas composition or temperature over the temperature interval below approximately 1550°K. At higher temperatures, however, the slope becomes more negative, and a change in majority carrier type occurs in the partial pressure region between 1 atm O_2 and $10^{-5.5}$ atm O_2. The conductivity is n-type at low temperatures and decreases with increasing oxygen partial pressure of the ambient gas, whereas at high temperature and near 1 atm O_2 the conductivity is p-type and increases with increasing oxygen partial pressure. The transition from n-type to p-type conductivity occurs at 1538°K for an ambient atmosphere of 1 atm O_2, and at increasing temperatures as the oxygen partial pressure in the ambient gas decreases. Measurements on two samples agreed to within 8% in the low temperature range. The data in the high temperature was less reliable because of rapid decomposition of the sample in low oxygen partial pressure gases, and because of thermochemical reactions between the sample and the platinum contacts.

The electrical conductivity data indicates a transition from intrinsic to extrinsic control of the conduction process as the temperature is lowered. The effect of aliovalent impurities on the conduction process is often observed when the temperature is lowered to the point where the concentration of thermally generated defects

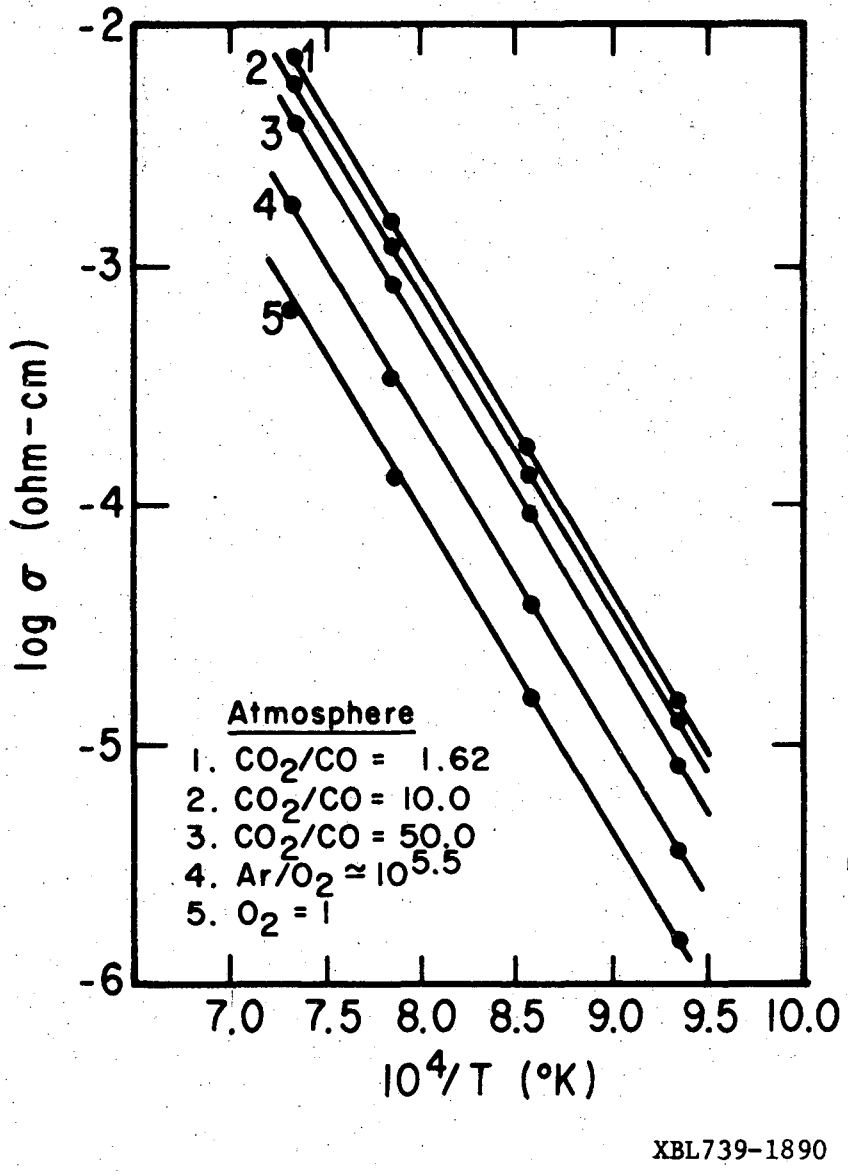

Figure 3. Dependence of the electrical conductivity on reciprocal temperature for fixed oxygen buffer gases

becomes comparable to that of aliovalent impurities. Below this temperature the conduction process becomes dominated by the fixed impurity concentration. The conduction mechanism for the lower temperature slope is attributed to impurity or intrinsic-type conduction through interstitial ions, and the high temperature slope attributed to intrinsic-type conduction associated with anion vacancies.

High Temperature Conduction Range

If the defects structure of $Gd_3Gd_5O_{12}$ behaves as a simple sesquioxide, A_2O_3, and if the effect of decreasing oxygen pressure is to create anion vacancies in the lattice, then the predominent defect formation reaction is

$$O = \frac{1}{2} O_{2(g)} + O_v^{n+} + ne^- \qquad (1)$$

with the equilibrium constant,

$$K_1 = \left[O_v^{n+}\right][e^-]^n P_{O_2}^{1/2} . \qquad (2)$$

The simplified electroneutrality condition is

$$[e^-] = n\left[O_v^{n+}\right] \qquad (3)$$

and the electrical conductivity expression becomes,

$$\sigma = q\mu_e[e^-] = q\mu_e\left[nK_1 P_{O_2}^{-1/2}\right]^{(1+n)^{-1}} \qquad (4)$$

where q and μ_e are the electronic charge and mobility, respectively.

The standard enthalpy of formation for this nonstoichiometric defect reaction, ΔH_1^o, is related to the equilibrium constant by the well-known expression,

$$K_1 \alpha \exp\left(\Delta S_1^o/k\right) \exp\left(-\Delta H_1^o/kT\right) . \qquad (5)$$

If the electronic mobility μ_e is essentially independent of temperature, then ΔH_1^o can be calculated from the expression,

$$\Delta H_1^o = -(1 + n) \frac{d \ln \sigma}{d(1/T)} . \qquad (6)$$

The oxygen vacancy charge n was determined from the conductivity dependence on oxygen partial pressure, Eq. 4. The measurements obtained in this study show that σ varies as $P_{O_2}^{-1/\gamma}$ with $\gamma \simeq 6$ in the temperature range between 1550°K and 1650°K, but at higher temperature the coefficient γ decreased toward 5. This change is possibly influenced by decomposition of the sample and to reactions between the sample and the Pt electrodes in the low oxygen partial pressure range. For the temperature range in which $\gamma = 6$ the oxygen vacancy charge state is $n = 2$ and the activation enthalpy for the defect function reaction, Eq. 1, is found to be $\Delta H_1^o \simeq 5$ eV .

Similar results have been reported for rare earth sesquioxides (10). Tare and Schmalzreid (5) have reported n-type conduction in

Sm_2O_3 on the basis of emf measurements at low P_{O_2} pressures. Schwab and Bohla (11) and also Tallan and Vest (12) found similar evidence for n-type conductivity in Eu_2O_3 and Y_2O_3 and confirm the $P_{O_2}^{-1/6}$ dependence of the conductivity.

The dependence of conductivity on $P_{O_2}^{-1/\gamma}$ where $\gamma < 6$ can indicate that several defect types are present. The value of γ equal to 6 is strictly true only for a parabolic conduction band model with nondegenerate carrier concentration. The theory of heavily doped semiconductors, however, predicts that the donor ionization energy decreases with donor concentration (13), and this effect has been observed in Ge (14). Also, studies of nonstoichiometric $Ce_{1+x}O_2$ have shown that a combination of singly and doubly ionized oxygen vacancies, or quadruply ionized cerium interstitials give rise to $\gamma = 5$, whereas singly ionized oxygen vacancies or triply ionized cerium interstitials cause $\gamma = 4$ (15).

Low Temperature Conduction Range

The logarithm of the electrical conductivity of $Gd_3Ga_5O_{12}$ in the low temperature range is shown in Fig. 3 as a function of reciprocal absolute temperature. The phenomenological activation enthalpy in this temperature range is

$$\Delta H_1^o = - \frac{d \ \ell n \ \sigma}{d(1/T)} . \qquad (7)$$

The activation enthalpy for the data in Fig. 3 was found to be

2.60 ± 0.11 eV , independent of the buffer gas composition.

The isothermal dependence of $\log \sigma$ on the logarithm of the oxygen partial pressure was determined by calculating the oxygen partial pressure for each ambient gas mixture at specific temperatures, and these data are shown in Fig. 4. The isothermal variation of σ with P_{O_2} at the fixed temperatures can be expressed by the following equations:

$$\sigma(T = 1073^{\circ}K) = 1.622 \times 10^{-6} P_{O_2}^{-(19.18)^{-1}}$$

$$\sigma(T = 1173^{\circ}K) = 1.748 \times 10^{-5} P_{O_2}^{-(15.97)^{-1}}$$

$$\sigma(T = 1273^{\circ}K) = 1.373 \times 10^{-4} P_{O_2}^{-(13.29)^{-1}} \qquad (8)$$

$$\sigma(T = 1373^{\circ}K) = 6.456 \times 10^{-4} P_{O_2}^{-(11.47)^{-1}}$$

If σ is expressed as a function of $P_{O_2}^{-1/\gamma}$, then γ varies from 19.18 to 11.47 in the above temperature range. Therefore, the conductivity in this range is n-type, but relatively insensitive to oxygen partial pressure. It should be noted that a dependence of σ on $P_{O_2}^{-1/\gamma}$ where γ is much greater than 6 has been observed in other high band-gap oxides. The value of γ measured for CdO ranges between 6 and 14 (16-18).

Changes in the activation energy for electronic conductivity with decreasing temperature are usually associated with the effects of aliovalent impurities on the prevailing defect equilibrium required

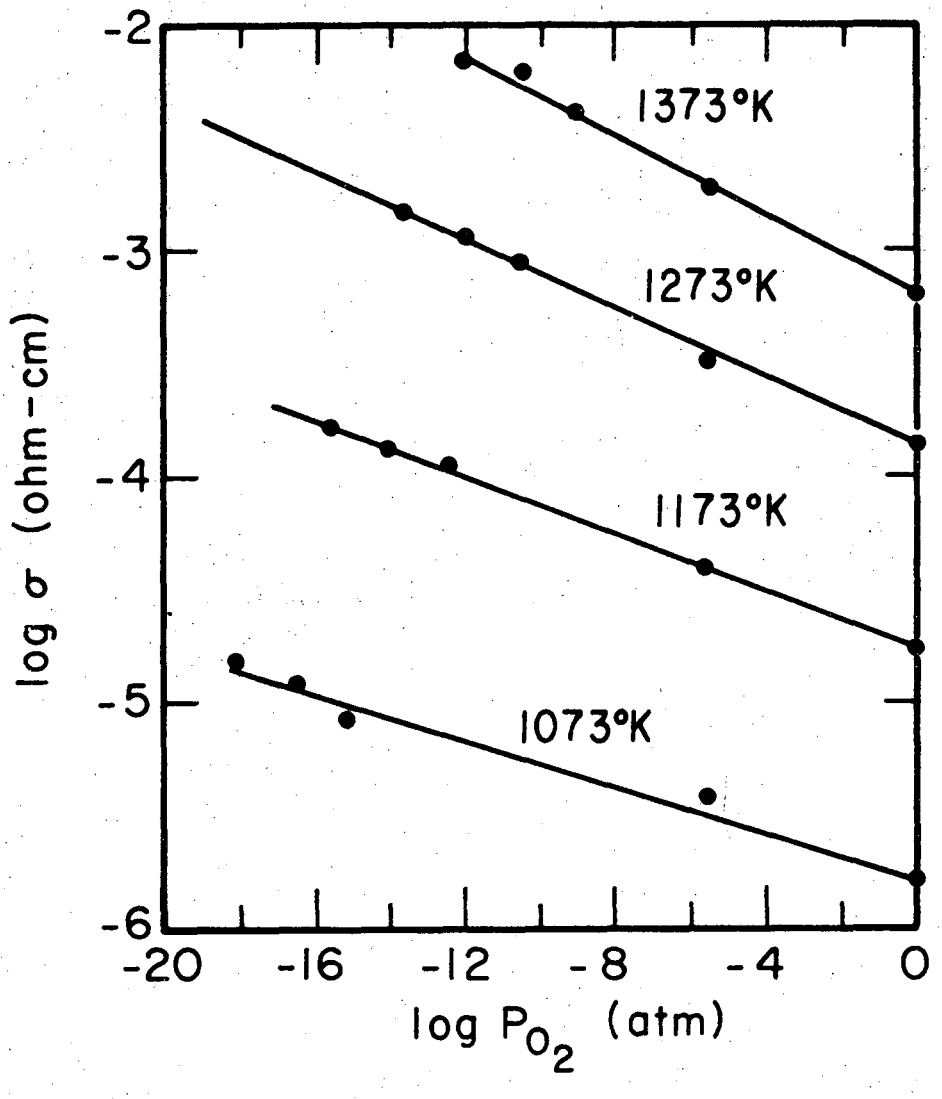

XBL739-1891

Figure 4. Isothermal dependence of the electrical conductivity on oxygen partial pressure

for electroneutrality in the crystal. Aliovalent impurities were not detected in the experimental sample by emission spectrographic analysis, although these impurities could still be present at levels below the limit of detectability by this method. The only detected impurity, aluminum, is not aliovalent.

The Gd : Ga rate in the crystal is expected to give rise to the observed low temperature slope of $\log \sigma$ versus $1/T$ by the introduction of interstitial cations, or cation vacancies into the crystal. Only interstitial cations will produce the observed n-type conductivity, however; and based on ionic radii a stoichiometric excess of Ga^{3+} or Ga^{1+} interstitials is most likely. Similarly, the aluminum impurity would be expected to occupy interstitial sites.

A non-stoichiometric excess of Ga_2O_3 is added to the melt for Czochralski crystal growth of $Gd_3Ga_5O_{12}$ to compensate for the dissociation of Ga_2O_3 into $Ga_2O_{(9)}$ and $O_{2(9)}$ at the melting point, 2023 °K, a major problem in the crystal growth of this compound. Witter (19) has used the measurements of Frosh et al. (20) on the partial pressure of Ga_2O in equilibrium with Ga_2O_3 and $Ga_{(\ell)}$ to estimate the oxygen partial pressure (.003 atm) which will minimize Ga_2O loss during crystal growth. Nielsen, however, has reported that successful crystal growth of $Gd_3Ga_5O_{12}$ requires 0.02 atm O_2 (21). Therefore, the non-stoichiometric gallium content should decrease along the $Gd_3Ga_5O_{12}$ crystal.

If Ga^{3+} or $A\ell^{3+}$ interstitial ions are present in the lattice in excess of the ionized anion vacancies produced by defect formation

reaction Eq. 1, then the electroneutrality condition is

$$3\left[Ga_I^{3+}\right] + 3\left[A\ell_I^{3+}\right] = [e^-] \tag{9}$$

and the extrinsic n-type conductivity expression,

$$\sigma = 3q\mu_e\left\{\left[Ga_I^{3+}\right] + \left[A\ell_I^{3+}\right]\right\} \tag{10}$$

is independent of P_{O_2} until a sufficiently low oxygen partial pressure is reached that anion vacancies dominate the charge neutrality condition. Attempts were made to deduce defect mechanisms which yield values of γ in the range of 11 to 20, but these remain speculative. It is also possible that the observed variation in σ in the low temperature region is caused by a dependence of the mobility μ_e on the anion vacancy concentration.

A schematic representation of the dependence of the electrical conductivity on inverse absolute temperature and oxygen partial pressure is shown in Fig. 5. The total conductivity is derived from extrinsic, electronic and hole conduction mechanisms in different regions of $\left(1/T, P_{O_2}\right)$ space. The total extrinsic conductivity, σ_{ext}, is independent of P_{O_2} in the ideal, whereas the electron and hole conductivities $\sigma_\ominus$ and $\sigma_\oplus$ are proportional to $P_{O_2}^{-1/\gamma}$ and $P_{O_2}^{+1/\gamma'}$, respectively at constant temperature. All three conduction modes exhibit an Arrhenius-type temperature dependence at constant P_{O_2}, with apparent activation enthalpies ΔH_{ext}, $\Delta H_\ominus$ and $\Delta H_\oplus$ which are also independent of P_{O_2} and T. The total

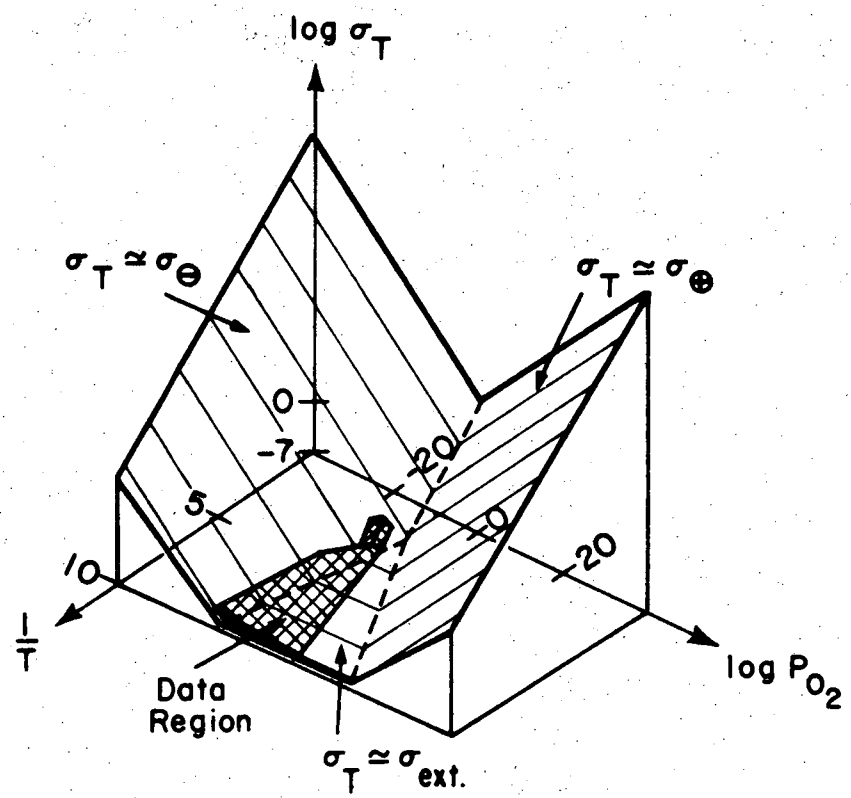

XBL739-1892

Figure 5. Schematic dependence of the logarithm of the total conductivity versus log P_{O_2} and $1/T$, with σ_{ext}, $\sigma_\ominus$ and $\sigma_\oplus$ representing extrinsic, electronic and hole conduction mechanisms

conductivity is then

$$\sigma_T = \sigma^0_{ext}\, e^{-\frac{\Delta H_{ext}}{kT}} + \sigma^0_{\ominus} P_{O_2}^{-1/\gamma}\, e^{-\frac{\Delta H_{\ominus}}{kT}} + \sigma^0_{\oplus} P_{O_2}^{1/\gamma'}\, e^{-\frac{\Delta H_{\ominus}}{kT}} . \qquad (11)$$

The experimentally measured conductivity data for $Gd_3Ga_5O_{12}$ is superimposed on Fig. 5 to show the high and low temperature regions and the change in conductivity type observed. From the properties of this diagram it is anticipated that a transition from extrinsic to intrinsic electron conduction should be observed at very low oxygen partial pressures, and that p-type hole conduction should be observable at oxygen pressures in excess of one atmosphere.

Acknowledgment

The financial support of the U.S. Atomic Energy Commission is gratefully acknowledged. The authors wish to thank Kenneth Geraghty for assistance in varifying the experimental measurements.

List of Figures

References

1. W.C. Dunlop, Jr., in "Methods of Experimental Physics: Solid State Physics," K. Lark-Horovitz and V.A. Johnson, Eds., Vol. 6, Part B, Academic Press, New York, 1959, p. 32.
2. D. L. Wood, J.P. Remeika, and E.D. Kolb, J. Appl. Phys., 41, 5315 (1970).
3. D.L. Wood and J.P. Remeika, J. Appl. Phys., 37, 1232 (1966).
4. F.A. Kröger, "The Chemistry of Imperfect Crystals," North-Holland Publishing Co., Amsterdam, The Netherlands, 1964.
5. V.B. Tare and H. Schmalzreid, Z. Phys. Chem. (NF), 43, 30 (1964).
6. W. Noddack and H. Walch, Z. Phys., 211, 194 (1959); Z. Electrochem., 63, 269 (1959).
7. R.R. Heikes, Rare Earth, 1, 247 (1961).
8. L.S. Karken and R.W. Gurry, J. Am. Chem. Soc., 67, 1398 (1945).
9. R.C. Weast, Ed., "Handbook of Chemistry and Physics," The Chemical Rubber Co., Cleveland, Ohio, 51st Edition, 1970-71, p. D-55.
10. T.H. Etsell and S.N. Flengas, Chem. Rev., 70, 339 (1970).
11. G.M. Schwab and F. Bohla, Z. Naturforsch. A, 23, 1549 (1968).
12. N.M. Tallan and R.W. Vest, J. Amer. Ceram. Soc., 49, 401 (1966).
13. V.L. Bonch-Bruyevich, "The Electronic Theory of Heavily Doped Semiconductors," American Elsevier Publishing Corp., New York, N.Y., 1966, Ch. 9.
14. W.W. Hervey, Phys. Rev., 123, 1666 (1961).
15. R.N. Blumenthal, P.W. Lee and R.J. Panlener, J. Electrochem. Soc., 118, 123 (1971).

16. E.F. Lamb and F.C. Tompkins, Trans. Faraday Soc., 58, 1424 (1962).

17. C.A. Hogarth, Nature, 167, 521 (1951).

18. F.P. Koffyberg, J. Solid State Chem., 2, 176 (1970).

19. D.E. Witter, Private communication.

20. C.J. Frosch and C.P. Thurmond, J. Phys. Chem., 66, 877 (1962).

21. J.W. Nielsen, Reported at the 17th Annual Conference on Magnetism and Magnetic Materials, November 1971.

TECHNICAL INFORMATION DIVISION
LAWRENCE BERKELEY LABORATORY
UNIVERSITY OF CALIFORNIA
BERKELEY, CALIFORNIA 94720